IOP PUBLISHING JOURNAL OF PHYSICS D: APPLIED PHYSICS

J. Phys. D: Appl. Phys. **42** (2009) 075410 (5pp) doi:10.1088/0022-3727/42/7/075410

Heteroepitaxial growth and luminescence properties of non-polar (1 1 0) orientation ZnO films on Si(0 0 1) substrates by pulsed laser deposition

Y W Zhang[1,4], X M Li[1,5], W D Yu[1], C Yang[1,4], X Cao[1,4], X D Gao[1], J F Kong[2], W Z Shen[2], J L Zhao[3] and X W Sun[3]

[1] State Key Laboratory of High Performance Ceramics and Superfine Microstructures, Shanghai Institute of Ceramics, Chinese Academy of Sciences, Shanghai 200050, People's Republic of China
[2] Laboratory of Condensed Matter Spectroscopy and Opto-Electronic Physics, Department of Physics, Shanghai Jiao Tong University, Shanghai 200030, People's Republic of China
[3] School of Electrical and Electronic Engineering, Nanyang Technological University, Nanyang Avenue, Singapore 639798, Singapore
[4] Graduate School of the Chinese Academy of Sciences, Beijing 100039, People's Republic of China

E-mail: lixm@mail.sic.ac.cn

Received 3 November 2008, in final form 5 February 2009
Published 13 March 2009
Online at stacks.iop.org/JPhysD/42/075410

Abstract

Epitaxial growth of a ZnO(1 1 0)/STO(0 0 1)/TiN(0 0 1)/Si(0 0 1) heterostructure has first been demonstrated on a Si(0 0 1) substrate by pulsed laser deposition. The growth process was monitored *in situ* by reflection high-energy electron diffraction, and the epitaxial orientation relationship was further confirmed by *ex situ* x-ray diffraction analysis. Results show that the high (1 1 0) oriented ZnO films are in domain-growth mode, and composed of two kinds of domains with their *c*-axes perpendicular to each other along STO⟨1 1 0⟩. The excitation-density-dependent photoluminescence spectra analyses at 83 K indicate that the ZnO films have good optical quality with low defect density, and no significant deep-level emission is detected. The strong near-band-edge luminescence consists of several acceptor-related emissions such as the acceptor–bound exciton emission (3.352 eV), the free electron–acceptor emission (3.318 eV) and the donor–acceptor-pair emission (3.248 eV). The presence of these acceptor-related emissions in undoped ZnO films should be attributed to structural acceptor defects, which are mainly caused by the domain-growth mode in this case.

(Some figures in this article are in colour only in the electronic version)

1. Introduction

Zinc oxide and its compounds are promising materials for broad optoelectronic applications, especially for blue/ultraviolet (UV) and white solid state light-emitting devices with superior advantages such as large exciton binding energy over III-nitride semiconductors [1–6]. As known, *c*-axis orientation is the preferred growth direction of ZnO on most currently available substrates. Unfortunately, this orientation causes a spontaneous and piezoelectric field within the active layers of ZnO-based light-emitting devices, resulting in low luminous efficiency [7, 8]. For better luminescence characteristics, non-polar ZnO is preferred [9, 10]. As commonly known, the epitaxial growth of non-polar ZnO has been achieved only on Al_2O_3 [11–13], MgO [14], $LaAlO_3$ [9, 10] and $SrTiO_3$ (STO) [15, 16] single-crystal substrates at present. However, its broad application in practical devices is not feasible due to the cost and small size of these single-crystal substrates [17]. Therefore, the heteroepitaxial growth

[5] Author to whom any correspondence should be addressed.

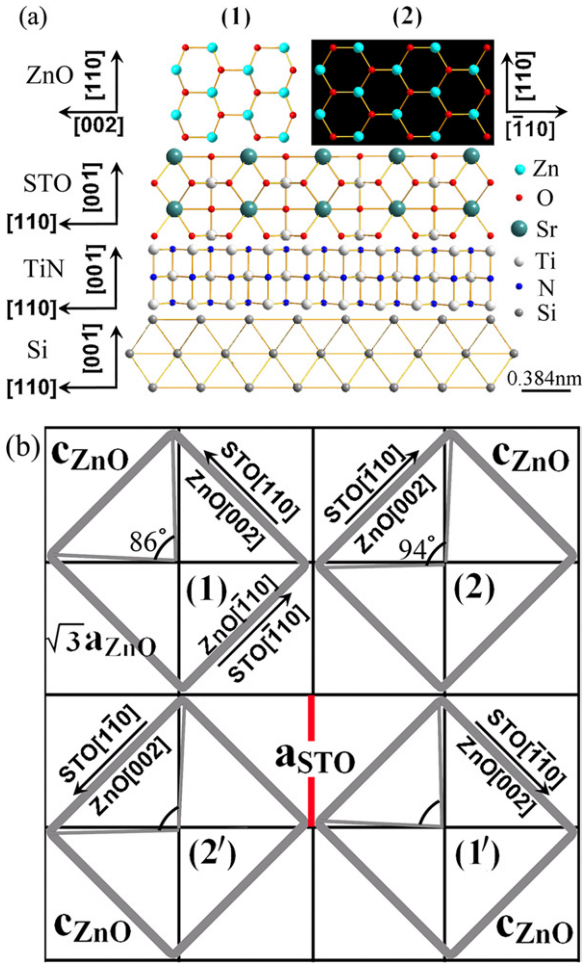

Figure 1. Schematic drawing of the epitaxial relationship of the multi-layer: ZnO(1 1 0)/STO(0 0 1)/TiN(0 0 1)/Si(0 0 1) viewing along $[1\,\bar{1}\,0]_{Si}$ direction (*a*); ZnO on STO(0 0 1) buffer viewing along $[0\,0\,1]_{STO}$ direction (*b*). The black thin and gray thick lines correspond to the unit cells of STO and ZnO, respectively.

of high-quality non-polar ZnO on silicon is very significant considering the superior performance in Si technology and the monolithic integration for large-scale optoelectronic devices [4]. Whereas, the acquirement of non-polar ZnO layer on Si substrate is not reported now due to a large lattice mismatch between ZnO and Si. To overcome this disadvantage, the buffer layer technique is a good route, and has been used widely in the semiconductor integration field.

As schematically illustrated in figure 1, high-quality epi-layers of the STO/TiN/Si(0 0 1) heterostructure can be fabricated throughout the domain epitaxial growth [18, 19]. Moreover, the epitaxial growth of non-polar ZnO(1 1 0) on STO(0 0 1) can be realized by two kinds of domain-match with the ZnO *c*-axes perpendicular to each other along $\langle 1\,1\,0\rangle_{STO}$ (figure 1), due to the small lattice mismatches between ZnO and STO of 2% and 6% for $\langle 1\,1\,0\rangle_{STO}$ along the directions of ZnO$[\bar{1}\,1\,0]$ and ZnO[0 0 2], respectively. In this paper, we first demonstrate the epitaxial growth of non-polar (1 1 0)-orientated ZnO films on the Si(0 0 1) substrate using the STO/TiN buffer by pulsed laser deposition (PLD). The growth behaviour, structural and optical properties of these non-polar ZnO films were investigated systematically.

2. Experimental details

The ZnO(1 1 0)/STO/TiN/Si(0 0 1) sample was entirely fabricated at a substrate temperature of 600 °C by PLD using a KrF excimer laser of 248 nm wavelength (Lambda Physik). Si(0 0 1) wafers were thoroughly cleaned to remove the surface native oxide layer before being loaded into the growth chamber. The target–substrate distance was optimized to 70 mm and the growth chamber was evacuated to the order of 10^{-5} Pa. Laser energy density and the laser frequency were set as 7 J cm^{-2} and 3 Hz. Firstly, a thin layer of TiN (∼10 nm) was then deposited on the Si(0 0 1), which helps to relax the mismatch between STO and Si and avoid the oxidation of the Si surface during the subsequent STO growth. Secondly, pure O_2 gas was introduced into the chamber and the pressure during the subsequent deposition was maintained at 1×10^{-2} Pa, laser energy density was set at 4 J cm^{-2}, STO films (∼40 nm) were grown *in situ*. Finally, a ZnO film (∼80 nm) was grown on STO/TiN/Si(0 0 1) at a laser energy density of 6 J cm^{-2}.

The orientation relations of the ZnO film were characterized by x-ray diffraction (XRD) θ–2θ and Φ-scan. The epitaxial relationship, surface morphology evolution and crystallinity were monitored *in situ* by reflection high-energy electron diffraction (RHEED). Low-temperature (LT) photoluminescence (PL) spectroscopy measurements were performed at the installation (Jobin Yvon LabRAM HR 800UV), excited by the 325 nm line of a He–Cd laser and measured at 83 K.

3. Results and discussion

In the θ–2θ measurement (figure 2(*a*)), the sample performs high ZnO(1 1 0)//STO(0 0 2)//TiN(0 0 2) orientation, as we expect. However a tiny ZnO(0 0 2) orientation XRD peak is also observed, indicating that there is very little other domain structure in the film. From the Φ-scan pattern of ZnO(1 0 1) in figure 2(*b*), four pairs of split peaks with about 4° split angle are adjacent at 90° intervals, which confirms that the (1 1 0) rectangular surface cell has a four-fold symmetry due to two kinds of in-plane orientation growth on the square lattice of STO(0 0 1), as illustrated in figure 1(*b*). This epitaxial relationship of ZnO(1 1 0) on STO(0 0 1) is similar to that of ZnO(1 1 0) on $LaAlO_3$(0 0 1), which can be described as ZnO[0 0 2] ∥ STO⟨1 1 0⟩ and ZnO$[\bar{1}\,1\,0]$ ∥ STO$\langle\bar{1}\,1\,0\rangle$ [9]. If the non-centro-symmetry of ZnO is taken into consideration, the positive c-axis direction is not equal to the negative c-axis direction, and the domain (1), (2) is not equal to the domain (1′), (2′). However, the XRD cannot identify the difference between them. Therefore, there are only two sets of ZnO{1 0 1} peaks appearing in the Φ-scan. From the geometric relationship, the φ angle of ZnO{1 0 1} is determined by projecting the plane normal of ZnO{1 0 1} on a surface parallel to ZnO(1 1 0). From the calculation, the φ angles between the ZnO{1 0 1} peaks are alternated by 86° and 94°. It is now clear that the 4° split angle is the result of two sets of ZnO{1 0 1} with 90° rotation relative to each other. Therefore the explanation of the ±2° misalignment of ZnO(1 1 0) with STO(0 0 1) is not necessary for the 4° split angle [15, 16].

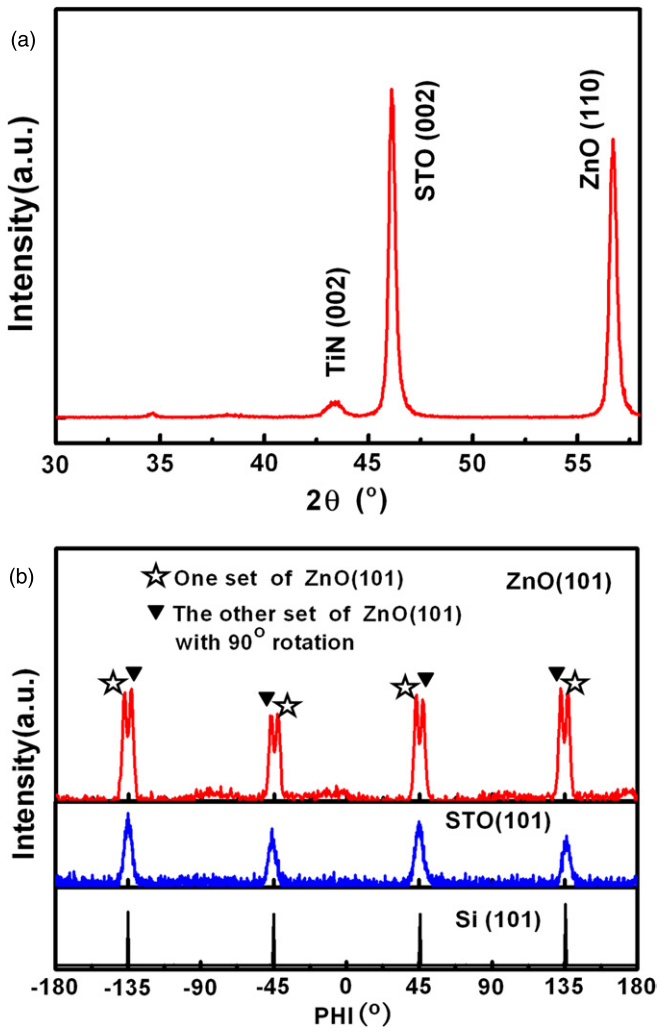

Figure 2. XRD spectra of the epitaxial ZnO samples on STO/TiN buffered Si(0 0 1): θ–2θ scan (*a*), and Φ-scans showing two sets of ZnO(1 0 1) peaks, STO(1 0 1) peaks and Si(1 0 1) peaks (*b*).

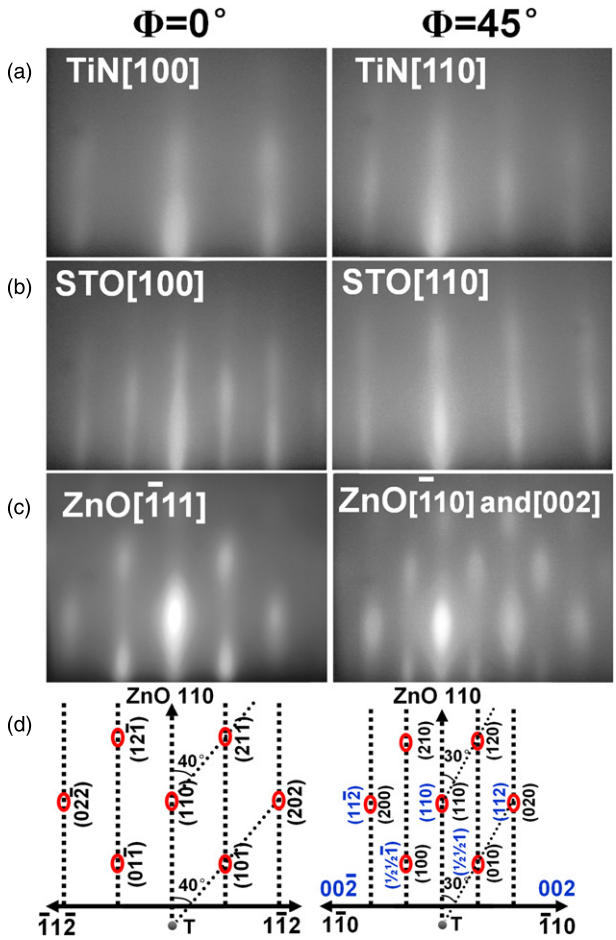

Figure 3. Evolution of RHEED patterns during the epitaxial growth on Si(0 0 1): TiN buffer layer (*a*), STO buffer layer (*b*), ZnO layer (*c*), by the electron beam incident azimuth along $[1\,0\,0]_{Si}(\Phi = 0^\circ)$ and $[1\,1\,0]_{Si}(\Phi = 45^\circ)$. Order stripes with spots observed in (*c*) correspond to the sections of reciprocal lattice rods and spots intersected by Ewald sphere, which are schematically plotted in (*d*).

Furthermore, the ZnO/STO/TiN growth details can be conveniently observed by *in situ* RHEED. Figure 3 shows typical RHEED patterns of TiN, STO and ZnO by the electron beam incident azimuth along $[1\,0\,0]_{Si}(\Phi = 0^\circ)$ and $[1\,1\,0]_{Si}(\Phi = 45^\circ)$. The sharp streaky RHEED patterns from the TiN and the STO buffer layers (figures 3(*a*) and (*b*)) indicate the atomically flat buffers formed through the layer-by-layer epitaxial growth with the in-plane epitaxial relationship of STO[1 0 0] ‖ TiN[1 0 0] ‖ Si[1 0 0], as confirmed by XRD. When ZnO layer growth begins, several Bragg-reflection spots are superposed on the sharp streak diffraction in figure 3(*c*), implying that the film has grown in the Stranski–Krastanov growth mode. These streaky patterns can be observed four times by rotating the film around its normal for 360° ($\Phi = 0^\circ$–360°). This four-fold symmetry further indicates in-plane alignment of epitaxial ZnO[0 0 2] ‖ STO⟨1 1 0⟩ and ZnO[$\bar{1}$ 1 0] ‖ STO⟨$\bar{1}$ 1 0⟩ corresponding to the two kinds of domains with their c-axes perpendicular to each other along STO⟨1 1 0⟩ [9, 15]. To understand the diffraction pattern clearly, the order stripes with spots observed in figure 3(*c*) are schematically plotted in figure 3(*d*), which correspond to the sections of reciprocal lattice rods and spots intersected by the Ewald sphere. Moreover, the diffraction spots can be identified as the Bragg-lattice spots of the relevant crystal planes through calculation of crystal plane azimuth and spacing, as shown in figure 3(*d*) [9], and the spots in figure 3(*c*) of $\Phi = 45^\circ$ can be regarded as two set Bragg spots due to the two kinds of in-plane alignment of epitaxial ZnO[0 0 2] ‖ STO[1 1 0] and ZnO[$\bar{1}$ 1 0] ‖ STO[1 1 0]. From the calculation, the angles between the planes of ZnO(1 0 1) versus (1 1 0), ZnO(0 1 0) versus (1 1 0) and ZnO(1 1 2) versus (1 1 0) are about 40°, 30° and 30°, which are in good agreement with the spatial arrangement of the diffraction spots in figure 3(*c*). The consistency of these structural analyses above clearly indicates that the epitaxial relationship of the ZnO(1 1 0)/STO(0 0 1)/TiN(0 0 1)/Si(0 0 1) heterostructure is just as we expect and is illustrated in figure 1.

The LT PL measurements were carried out at 83 K to investigate the luminescence properties and the defect structure of these films. The test results are similar to the room-temperature photoluminescence characteristics of the samples: no significant deep-level emission (DLE) such

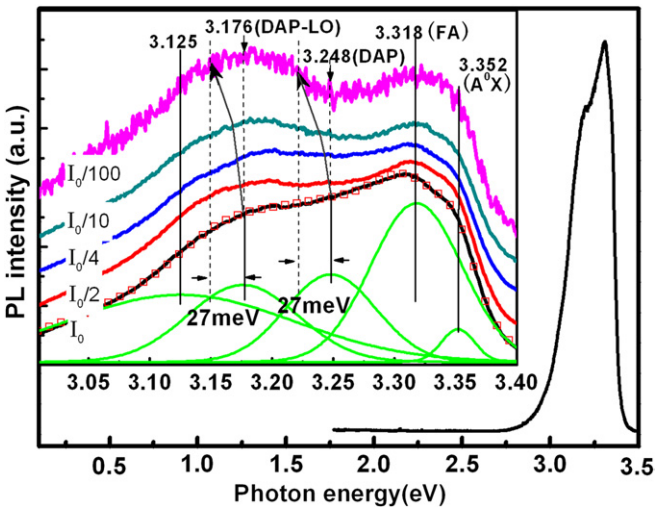

Figure 4. PL spectra from the ZnO epi-layer measured at 83 K. The inset shows the excitation-density-dependent PL spectra for the ZnO film at 83 K.

as a green band is detected (figure 4), whereas a strong near-band-edge (NBE) emission is observed, indicating good optical quality of the films. Moreover, it is interesting that the feature of this NBE emission is similar to the characteristic of ultraviolet emission observed in many p-type doped ZnO materials [20–23]. To further understand this emission, the excitation-density-dependent LT PL was examined and the multi-Gaussian fittings to the spectra have been performed, as shown in the inset of figure 4. The best fitting result consists of five bands at 3.352, 3.318, 3.248, 3.176 and 3.125 eV under the excitation density of $I_0 = 1.25\,\mathrm{kW\,cm^{-2}}$. The former three peaks were observed and identified as neutral acceptor–bound exciton (A^0X) emission, free electrons to neutral acceptor (FA) transition and donor–acceptor pair (DAP) emission, respectively, in N-, P-, As-, Sb-doped ZnO research [20–23]. In addition, the peak at 3.125 eV is usually attributed to the native defect of zinc vacancy (V_{Zn}) [24]. It seems difficult to understand the substantive appearance of acceptor-related emission in undoped ZnO. However, this phenomenon can be explained by localized-acceptors relative to structural defects such as stacking faults. Schirra *et al* give clear evidence that localized-acceptors causing the 3.31 eV (FA) emission are located in basal plane stacking faults [25]. From the structural analyses above, the ZnO films in our study are in the two kinds of in-plane orientation-growth mode, which could easily induce structural defects at the domain-boundary. Therefore the acceptor-related emissions are probably produced through these structural acceptor defects. Moreover, the binding energy of an acceptor E_A can be calculated from FA with [26]

$$E_A = E_g - E_{FA} + k_B T/2, \tag{1}$$

where E_{FA} is the peak energy of free electrons to neutral acceptor (FA) transition. With a fundamental band gap energy of $E_g = 3.437$ eV [22, 26], the value of E_A is then calculated to be 122 meV, which is close to the value of $E_A = 130$ meV deduced from the FA fitting by Schirra *et al* [25].

The emission at 3.176 eV should be the first-order longitudinal optical (DAP-LO) phonon replica of DAP (3.248 eV) with an energy difference of 72 meV. As seen from the inset of figure 4, the emissions at 3.248 and 3.176 eV show a 27 meV red-shift under lower excitation density, while the other emissions perform no obvious peak-shift. This phenomenon can be used to prove our assignments of the DAP-related emissions. The energy of the DAP luminescence is represented as follows [27]:

$$E_{DAP} = E_g - E_D - E_A + e^2/4\pi\varepsilon r, \tag{2}$$

where E_{DAP}, E_g, E_D, E_A, ε and r are peak energies of DAP transition, fundamental band gap energy, donor binding energy, acceptor binding energy, dielectric constant and an average DAP distance. It is well known that as the excitation power decreases, fewer photo-excited DAP are created, resulting in a larger average DAP distance r [28]. Thus DAP emissions show a typical red-shift as the excitation power decreases. Assuming a homogeneous distribution of donors and acceptors, this leads to [25]:

$$N_{A/D} = 3/[4\pi(r)^3], \tag{3}$$

where the $N_{A/D}$ is the majority impurity concentration. Since the FA transition is stronger in intensity than the DAP line, the acceptor concentration exceeds the donor concentration. With an average donor binding energy of $E_D = 90$ meV [21], an acceptor binding energy $E_A = 122$ meV as derived above, the majority impurity N_A was estimated to be $=6.2 \times 10^{17}\,\mathrm{cm^{-3}}$ from equations (2) and (3). Although there are two types of orthogonal domains in the formation of non-polar ZnO(1 1 0) films on STO/TiN buffered Si, the optical quality of the ZnO films is very good with low defect density.

4. Conclusions

In summary, epitaxial growth of non-polar (1 1 0)-orientation ZnO on a STO/TiN-buffered Si(0 0 1) substrate has been demonstrated using pulsed laser deposition. On the smooth surface of STO(0 0 1) buffer layers, ZnO films are preferred to form a four-fold symmetric structure, resulting from two kinds of in-plane domain-growth with the ZnO c-axes perpendicular to each other along STO⟨1 1 0⟩. The LT PL spectra analyses indicate that the ZnO films have good optical quality and no significant DLE is detected from the ZnO films. The strong NBE luminescence is composed of several acceptor-related emissions owing to structural acceptor defects, which are caused mainly by the domain-growth mode. These results indicate that the all-epitaxial technology may be a good route to obtain high-quality non-polar ZnO films on a Si substrate, and further study will be meaningful to the application and mechanism of ZnO material.

Acknowledgments

Financial support is acknowledged from the Ministry of Science and Technology of People's Republic of China through 973 National Natural Science Foundation (No 2009CB623304).

References

[1] Tsukazaki A *et al* 2005 *Nature Mater.* **4** 42
[2] Yang C, Li X M, Gu Y F, Yu W D, Gao X D and Zhang Y W 2008 *Appl. Phys. Lett.* **93** 112114
[3] Ryu Y R, Lubguban J A, Lee T S, White H W, Jeong T S, Youn C J and Kim B 2007 *J. Appl. Phys. Lett.* **90** 131115
[4] Feng X, Kang, J, Inami W, Yuan X L, Terauchi M, Sekiguchi T, Tsunekawa S, Ito S and Sakurai T 2007 *Cryst. Growth Des.* **7** 564
[5] Sun X W, Zhao J L, Tan S T, Tan L H, Tung C H, Lo G Q, Kwong D L, Zhang Y W, Li X M and Teo K L 2008 *Appl. Phys. Lett.* **92** 111113
[6] Zhang Y W *et al* 2008 *J. Phys. D: Appl. Phys.* **41** 205105
[7] Waltereit P, Brandt O, Trampert A, Grahn H T, Menniger J, Ramsteiner M, Reiche M and Ploog K H 2000 *Nature* **406** 865
[8] Im J S, Kollmer H, Off J, Sohmer A, Scholz F and Hangleiter A 1998 *Phys. Rev.* B **57** R9435
[9] Tian J S, Liang M H, Ho Y T, Liu Y A and Chang L 2008 *J. Cryst. Growth* **310** 777
[10] Ho Y T, Wang W L, Peng C Y, Liang M H, Tian J S, Lin C W and Chang L 2008 *Appl. Phys. Lett.* **93** 121911
[11] Zhang B P, Segawa Y, Wakatsuki K, Kashiwaba Y and Haga K 2001 *Appl. Phys. Lett.* **79** 3953
[12] Moriyama T and Fujita S 2005 *Japan. J. Appl. Phys.* **44** 7919
[13] Saraf G, Lu Y and Siegrist T 2008 *Appl. Phys. Lett.* **93** 041903
[14] Cagin E, Yang J, Wang W, Phillips J D, Hong S K, Lee J W and Lee J Y 2008 *Appl. Phys. Lett.* **92** 233505
[15] Wei X H, Li Y R, Zhu J, Huang W, Zhang Y, Luo W B and Ji H 2007 *Appl. Phys. Lett.* **90** 151918
[16] Bellingeri E, Marre D, Pallecchi I, Pellegrino L, Canu G and Siri A S 2005 *Thin Solid Films* **486** 186
[17] Chen T L, Li X M, Yu W D and Zhang X 2005 *Appl. Phys.* A **81** 657
[18] Zheleva T, Jagannadham K and Narayan J 1994 *J. Appl. Phys.* **75** 860
[19] Vispute R D, Narayan J, Dovidenko K, Jagannadham K, Parikh N, Suvkhanov A and Budai J D 1996 *J. Appl. Phys.* **80** 6720
[20] Jiao S J, Lu Y M, Shen D Z, Zhang Z Z, Li B H, Zheng Zh H, Yao B, Zhang J Y, Zhao D X and Fan X W 2007 *J. Lumin.* **122–123** 368
[21] Ye J D, Gu S L, Li F, Zhu S M, Zhang R, Shi Y, Zheng Y D, Sun X W, Lo G Q and Kwong D L 2007 *Appl. Phys. Lett.* **90** 152108
[22] Hwang D K, Kim H S, Lim J H, Oh J Y, Yang J H, Park S J, Kim K K, Look D C and Park Y S 2005 *Appl. Phys. Lett.* **86** 151917
[23] Xiu F X, Yang Z, Mandalapu L J, Zhao D T and Liu J L 2005 *Appl. Phys. Lett.* **87** 252102
[24] ZengY J, Ye Z Z, Xu W Z, Lu J G, He H P, Zhu L P, Zhao B H, Che Y and Zhang S B 2006 *Appl. Phys. Lett.* **88** 262103
[25] Schirra M, Schneider R, Reiser A, Prinz G M, Feneberg M, Biskupek J, Kaiser U, Krill C E, Thonke K and Sauer R 2008 *Phys. Rev.* B **77** 125215
[26] Ryu Y R, Lee T S and White H W 2003 *Appl. Phys. Lett.* **83** 87
[27] Thomas D G, Gershenzon M and Trumbore F 1964 *Phys. Rev.* A **133** A269
[28] Tamura K *et al* 2003 *Solid State Commun.* **127** 265